Rev. LatinAm. Metal. Mat.

Artículo Regular

www.rlmm.org

MAGNETIC SUSCEPTIBILITY FOR THE Cu_2-II-IV-S_4 (II=Mn, Fe; IV=Si, Ge or Sn) COMPOUNDS: EXCHANGE INTERACTION PARAMETERS

M. Quintero[1], E. Quintero[1], E. Moreno[1], P. Grima-Gallardo[1,2], J. Marquina[3], S. Alvarez[1,3], C. Rincón[1], D. Rivero[1], M. Morocoima[1], J. A. Henao[4], M. A. Macías[4], J. M. Briceño[5], N. Rodríguez[5,6]*

1: Centro de Estudios de Semiconductores (CES), Departamento de Física, Facultad de Ciencias, Universidad de los Andes, Mérida 5101, Venezuela. *2:* Centro Nacional de Tecnología Óptica (CNTO), Centro de Investigaciones de Astronomía (CIDA), Mérida 5101, Venezuela. *3:* Centro de Estudios Avanzados en Óptica (CEAO), Departamento de Física, Facultad de Ciencias, Universidad de los Andes, Mérida 5101, Venezuela. *4:* Grupo de investigación en Química Estructural (GIQUE), Facultad de Ciencias, Escuela de Química, Universidad Industrial de Santander, Apartado aéreo 678, Bucaramanga, Colombia. *5:* Laboratorio de Análisis Químico y Estructural de Materiales, Departamento de Física, Universidad de Los Andes, Mérida 5101, Venezuela. *6:* Departamento de Ciencias, Área de Física, Núcleo Bolívar, Universidad de Oriente, Venezuela.

**e-mail: peg@ula.ve*

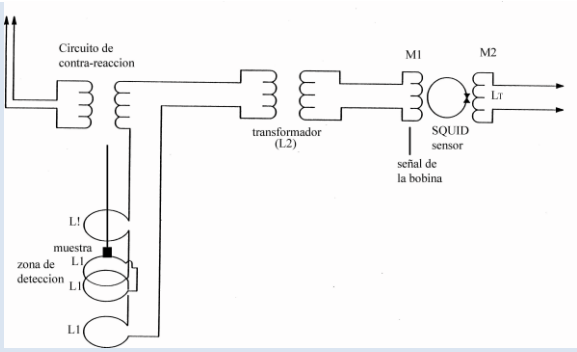

ABSTRACT

Measurements of magnetic susceptibility χ as a function of temperature (from 2 to 300 K) were made on polycrystalline samples of the compounds Cu_2MnSiS_4, Cu_2MnGeS_4, Cu_2MnSnS_4, Cu_2FeSiS_4 and Cu_2FeGeS_4. From the 1/ χ versus T curves, it was concluded that the samples were antiferromagnetic. These curves were also used to determine values of the Néel temperature T_N and the Curie-Weiss temperature θ for each compound. When the values of T_N and θ are plotted against its molecular weight W, it was found that the compounds containing Mn lie on the same straight line, while those with Fe lie on a different one. For each compound, an analysis was carried out in terms of the simple mean-field theory and using the virtual transition model of Geertsma *et al.* for exchange interaction, and values of exchange interaction parameters were determined from the measured T_N and θ data.

Keywords: magnetic semiconductor compound; magnetic properties; magnetic exchange interaction.

SUSCEPTIBILIDAD MAGNÉTICA DE LOS COMPUESTOS CU2-II-IV-S4 (II=MN, FE; IV=SI, GE O SN). PARÁMETROS DE LA INTERACCIÓN DE INTERCAMBIO

RESUMEN

Se realizaron medidas de la susceptibilidad magnética χ en función de la temperatura (2 a 300K) sobre muestras policristalinas de los compuestos Cu_2MnSiS_4, Cu_2MnGeS_4, Cu_2MnSnS_4, Cu_2FeSiS_4 y Cu_2FeGeS_4. De las curvas 1/ χ versus T, se concluye que las muestras fueron antiferromagnéticas. Estas curvas fueron también usadas para determinar los valores de la temperaturas de Néel T_N y de Curie-Weiss θ para cada uno de los compuestos. Cuando se grafican los valores de T_N y θ en función del peso molecular W, se encuentra que tanto los compuestos que contienen Mn como Fe muestran una dependencia lineal, pero con diferentes pendientes. Para cada compuesto, fue llevado a cabo un análisis en términos de la teoría de campo medio y el modelo de transición virtual de Geertsma *et al.* para la interacción de intercambio permitiendo la determinación de los valores de los parámetros de interacción a partir de los valores medidos de T_N y θ.

Palabras clave: compuestos semiconductores magnéticos; propiedades magnéticas; interacción magnética de intercambio.

1. INTRODUCTION

Quaternary magnetic semiconducting compounds of the I_2-II-IV-VI_4 type, where II = Mn, Fe or Co, IV = Si, Ge, Sn or Pb and VI = S, Se or Te, are of great interest because of their large magneto-optical effects which are observed due to the presence of paramagnetic ions [1-2]. As has been reported [2-4], most of these compounds showed either the tetrahedral tetragonal stannite ($I\bar{4}2m$) structure based on zinc-blende, and an orthorhombic superstructure derived from wurtzite (known as wurtz-stannite, $Pmn2_1$). It has been found recently that, at room temperature, Cu_2FeSnS_4 has a tetragonal crystal structure with space group $P\bar{4}$ [5]. All these structures are shown in figure 1.

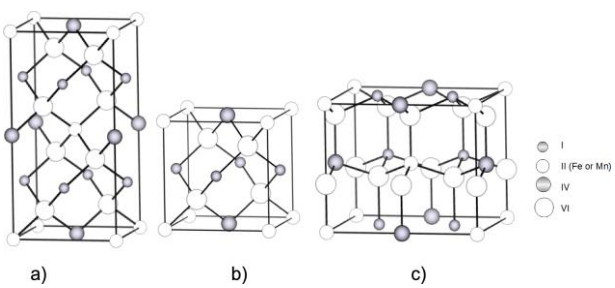

Figure 1. a) Tetragonal stannite $I\bar{4}2m$, b) pseudo-cubic $P\bar{4}$ and c) orthorhombic wurtz-stannite $Pmn2_1$ structures.

Results on the lattice parameter values and differential thermal analysis DTA for these materials have been reported lately in Ref. [6]. In a previous work [7], the magnetic behavior of some I_2-Mn-IV-Se_4 compounds has been published. However, the available information related to the magnetic behavior of I_2-(Mn,Fe)-IV-S_4 materials is very scarce. Hence, measurements of magnetic susceptibility χ as a function of temperature T in the range between 2 and 300 K have been carried out on the Cu_2MnSiS_4, Cu_2MnGeS_4, Cu_2MnSnS_4, Cu_2FeSiS_4 and Cu_2FeGeS_4 compounds. The magnetic results thus obtained were correlated with the details of the crystal structure to give values for the exchange interaction parameters for these compounds.

2. SAMPLE PREPARATION AND EXPERIMENTAL TECHNIQUES

The samples were produced by the melt and anneal technique. In each case, highly pure components (copper 99.98 %, manganese 99.97 %, iron 99.9 %, cobalt 99.99 %, silicon 99.999%, germanium 99.999%, tin 99.999 %, sulphur 99.997 % and/or selenium 99.9997 %) of 1 g sample were sealed under vacuum ($\approx 10^{-5}$ Torr) in a small quartz ampoule, and then the components were heated up to 200 °C and kept for about 1-2 h, then the temperature was raised to 500 °C using a rate of 40 K/h, and held at this temperature for 14 hour. After, the samples were heated from 500 °C to 800 °C at a rate of 30 K/h and kept at this temperature for another 14 hours. Then it was raised to 1150 °C at 60 K/h, and the components were melted together at this temperature. The furnace temperature was brought slowly (4 K/h) down to 600 °C, and the samples were annealed at this temperature for 1 month. Then, the samples were slowly cooled to room temperature using a rate of about 2 K/h. Magnetic susceptibility measurements as a function of T from 2 to 300 K were made using a Quantum Design MPMS-5 SQUID magnetometer with an external magnetic field of 1 x 10^{-2} T. Resulting $1/\chi$ versus T curves were analyzed to give various magnetic parameters, as discussed below.

3. RESULTS AND DISCUSSION

3.1 Magnetic Results

Measurements of zero-field cooling (zfc) (heating curve) and field cooling (fc) (cooling curve) magnetic susceptibility were made on the samples and typical obtained $1/\chi$ vs T curves are shown in figs. 2a and 2b for Cu_2MnSnS_4 and Cu_2FeSiS_4 respectively.

The rest of the sample showed similar curves. It can be seen from these figures that, for each compound, the $1/\chi$ vs T plot is linear at higher temperatures and the extrapolation of this line to $1/\chi=0$ gives a negative value of the Curie-Weiss θ indicating that these compounds are antiferromagnetic AF. It is also seen from these figures that, in each case, the susceptibility run under zero field cooling (zfc) is identical to the one obtained under field cooling (fc) condition, so that spin-glass behavior is ruled out here. Hence, almost ideal collinear antiferromagnetism is present for each compound. The Néel temperature T_N values for the materials

©2017 Universidad Simón Bolívar

can be obtained from the maximum peaks shown in the inset of figs. 2a and 2b.

For antiferromagnetic behavior, the variation of $1/\chi$ with T above the T_N is given by the relation [9],

$$1/\chi = (T-\theta)/C \quad (1)$$

where C the Curie constant and its theoretical value of C is given by [9]

$$C= N_A g^2 \mu_B^2 J(J+1)/3K_B W \quad (2)$$

N_A being the Avogadro number, μ_B the Bohr magneton and W the molecular weight of the compound. Thus, the $1/\chi$ vs T experimental data were fitted to eq. (1) and the resulting values of the magnetic parameter C and θ as well as values for T_N are listed in table 1, together with the lattice parameter values reported in earlier works for Cu_2FeSnS_4 [5], $Cu_2FeGeSe_4$ [8], $Cu_2MnSnSe_4$ [10], $Cu_2MnGeSe_4$ [11], and $Cu_2FeSnSe_4$ [11]. The variations of θ and T_N as a function of W of the material are shown in figs. 3a and 3b respectively.

As expected, it is observed from table 1 that for the Mn samples the experimental values of C_E are, close to the theoretical values of C_T obtained from eq. (2) using J=S=5/2, L=0 and g=2 for the Mn^{2+} ion. While for Cu_2FeSiS_4, Cu_2FeGeS_4 and Cu_2FeSnS_4 it is found that the value of C_E is close to the one obtained for C_T when the spin-only values (J=S=2, L=0 and g=2) are used in eq. (2) for the Fe^{2+} ion. This result would be due to the presence of crystal field effects and/or magnetic anisotropy which are responsible for the quenching of the orbital moment (L=0) in these samples. However, for $Cu_2FeGeSe_4$ and $Cu_2FeSnSe_4$, it is found that $C_E \approx C_T$ when L=S=2, J=4 and g=1.5 are used in eq. (2) for Fe^{2+}. This result would indicate that Fe^{2+} ions exhibit an orbital contribution to the magnetic moment which is also feasible in other materials involving Fe^{2+}.

It can be seen from fig. 3a that independent of the crystal structure of the sample, the values of θ for the Mn and Fe lay on different straight lines. It is also seen for the Mn samples that the variation of θ vs W is very small, i.e. $\theta \approx (-26 \pm 3)$ K, while for the Fe materials the absolute values of θ increase linearly as W is increased. These results would indicate that the values of θ for the Mn are not influence by the presence of diamagnetic cations contrary to that observed in the Fe samples. With regard to the variation of T_N with W it is seen from fig. 3b that the values of T_N for the Mn and most of the Fe materials lay on nearly parallel straight lines. It is also observed that Cu_2FeSnS_4 has a very large T_N value compared with the rest of the compounds. This would suggest that another straight line would exist for $P\bar{4}$ compounds. This behavior would be due to the smallest size of the pseudo-cubic $P\bar{4}$ structure, resulting in the highest magnetic interaction between the nearest magnetic neighbors.

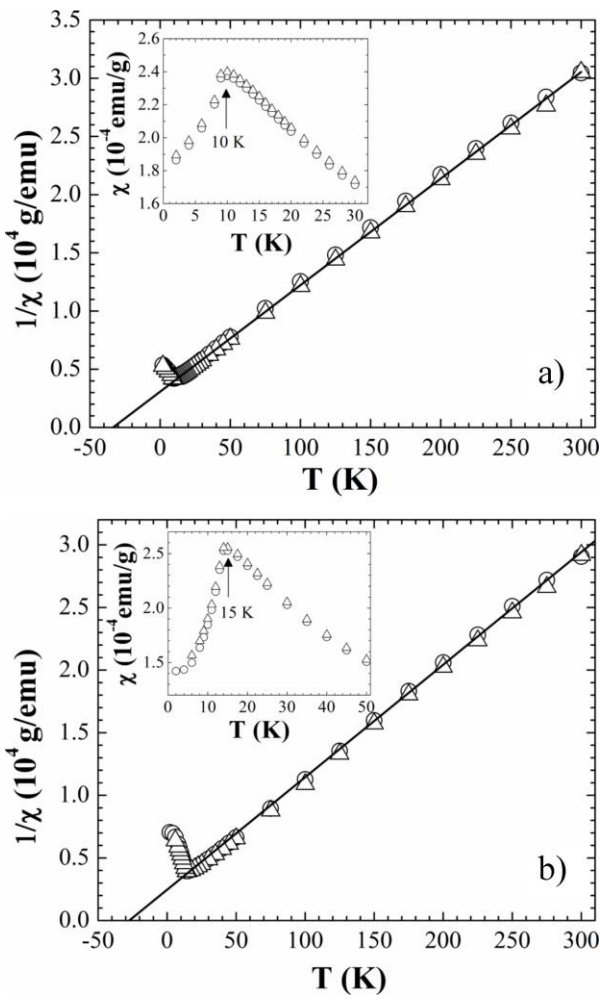

Figure 2. Typical curves of the reciprocal of susceptibility $1/\chi$ against temperature T for a) Cu_2MnSnS_4 and b) Cu_2FeSiS_4. Zero field cooling zfc: open circles, field cooling fc: open triangles. The Curie–Weiss behavior is represented by the solid line. Inset: temperature dependence of the magnetic susceptibility χ for a) Cu_2MnSnS_4 and b) Cu_2FeSiS_4 showing the Néel temperature T_N.

Table 1. Parameter values for antiferromagnetic Cu_2-II-IV-$S_4(Se_4)$ quaternary compounds. Experimental values of *a*, *b* and *c* taken from Ref. [7]. T_N and θ are the resulting Neel and Curie-Weiss temperatures. Resulting values of α and $-I_0/k$ and $-J_1/k$ obtained with u=2.

Nº	Compounds Space group	parameters (nm)	W (g/mol)	T_N (K)	θ_a (K)	C_T (x10^{-3}) (emu.g/K)	C_E (x10^{-3}) (emu.g/K)	Ref.		α (nm^{-1})	$-I_0/k$ (Knm^2)	$-J_1/k$ (K)
1	Cu_2MnSiS_4 $Pmn2_1$	a=0.7536 b=0.6442 c=0.6187	338.38	8	-29	12.9	11.5	Our	L=0 J=S=5/2	3.34	0.78	0.46
2	Cu_2MnGeS_4 $Pmn2_1$	a=0.7616 b=0.6513 c=0.6230	382.93	9	-20	11.4	11.4	Our	L=0 J=S=5/2	6.43	4.22	0.46
3	Cu_2MnSnS_4 $I\bar{4}2m$	a=0.5518 c=1.0807	429.00	10	-32	10.2	10.8	Our	L=0 J=S=5/2	3.74	1.31	0.55
4	Cu_2FeSiS_4 $Pmn2_1$	a=0.7421 b=0.6417 c=0.6141	339.28	15	-27	8.85	11.1	Our	L=0 J=S=2	8.88	31.37	1.05
5	Cu_2FeGeS_4 $I\bar{4}2m$	a=0.5336 c=1.0522	383.84	17	-48	7.8	8.0	Our	L=0 J=S=2	4.45	4.02	1.31
6	Cu_2FeSnS_4 $P\bar{4}$	a=0.5433 c=0.5410	429.91	38	-74	7.0	7.11	[6]	L=0 J=S=2	5.09	9.97	2.17
7	$Cu_2MnGeSe_4$ $Pmn2_1$	a=0.7996 b=0.6857 c=0.6572	570.51	10	-22	7.668	7.60	[12]	L=0 J=S=5/2	6.16	5.29	0.51
8	$Cu_2MnSnSe_4$ $I\bar{4}2m$	a=0.5766 c=1.1368	616.58	16	-25	7.09	6.60	[11]	L=0 J=S=5/2	9.57	59.99	0.72
9	$Cu_2FeGeSe_4$ $I\bar{4}2m$	a=0.5601 c=1.1056	571.42	20	-162	9.84	9.77	[9]	L=S=2 J=4	1.07	1.08	1.88
10	$Cu_2FeSnSe_4$ $I\bar{4}2m$	a=0.5705 c=1.1271	617.49	19	-200	9.11	10.00	[11]	L=S=2 J=4	0.56	0.78	1.75

3.2 Exchange Interaction Results

Another point of interest here is to discuss the exchange interaction parameters J_i in the present compounds. The mean field theory gives the following equations for θ and T_N [9]:

$$\theta = 2J(J+1)\,\Sigma m_i J_i/3k \qquad (3)$$

$$T_N = 2J(J+1)\,\Sigma \eta_i m_i J_i/3k \qquad (4)$$

where the summation is over sets of equidistant magnetic neighbors from a chosen magnetic atom, m_i, and J_i being the number and exchange interaction for the *i-th* set, *J* being the total angular moment and η_i being +1 for antiparallel and -1 for parallel spin. It was suggested in earlier work carried out on the Mn-III_2-VI_4 compounds [12] that a possible mechanism that explains the magnetic interaction between magnetic ions is the one proposed by Geertsma and Haas [13], based on the work of Concalves da Silva and Falicov [14]. This exchange interaction involves virtual transitions between the p-valence band and a band of d states arising from the magnetic ions, and the exchange parameter J_i can be taken to vary with distance r_i as

$$J_i = I_0 \exp(-\alpha r_i)/r_i^u \qquad (5)$$

where α depends on the effective mass of the valence band and the energy difference involved in the virtual transition. It has been shown that in the case of the Mn-III_2-VI_4 compounds [12] good results are obtained with u=2. If u=2 is used in the analysis, then, substituting eq. (5) into (3) and (4) one obtains

$$\theta/T_N = [\Sigma m_i \exp(-\alpha r_i)/r_i^2] \,/\, [\Sigma \eta_i m_i \exp(-\alpha r_i)/r_i^2] \qquad (6)$$

and the value of I_0/k can be determined from the following relation,

$$I_0/k = 3\theta/[2J(J+1)\Sigma m_i \exp(-\alpha r_i)/r_i^2] \qquad (7)$$

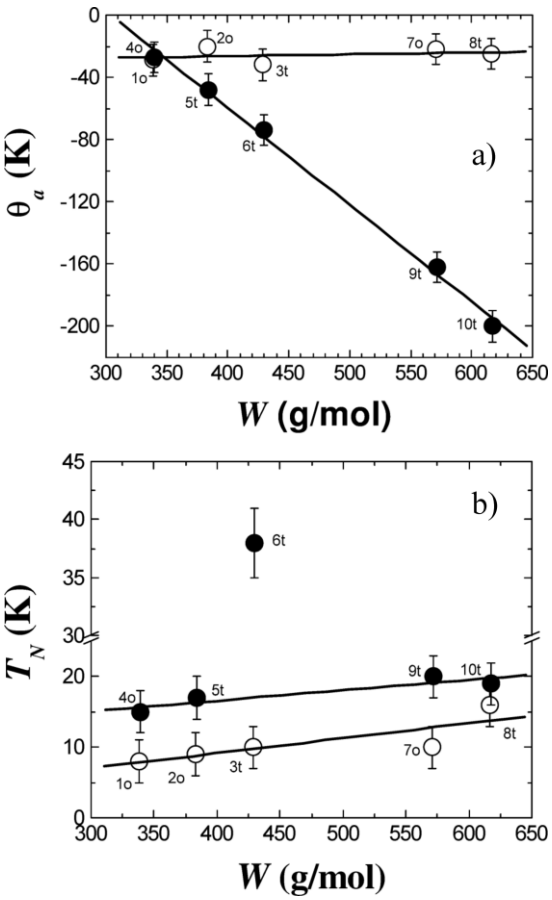

Figure 3. a) Dependence of the Curie-Weiss temperature θ with W. Open circles: compounds containing Mn; close circles: compounds containing Fe. The solid lines are to guide the eyes. b) Dependence of the Néel temperature T_N with W. Open circles: compounds containing Mn; close circles: compounds containing Fe. The solid lines are to guide the eyes.

It is seen that, in order to use equations (6) and (7) to calculate α and I_0, and so $J_i(r_i)$, it is necessary to know the configuration of the magnetic ions in the crystal structure as well as the orientation of the spins below the temperature T_N in the material. The magnetic structures for the materials are shown in figure 4, where for clarity only the magnetic cations are shown, and the value of i for equidistant magnetic cation position is also indicated. Choosing an origin on a magnetic atom site, the distances r_i between magnetic atoms is given by

$$r_i=[(u_ia/2)^2+(v_ia/2)^2+(w_ic/4)^2]^{1/2} \quad \text{for } I\bar{4}2m, \qquad (8)$$

$$r_i=[(u_ia)^2+(v_ia)^2+(w_ic)^2]^{1/2} \quad \text{for } P\bar{4}, \qquad (9)$$

$$r_i=[(u_ia/2)^2+(v_ib/3)^2+(w_ic/2)^2]^{1/2} \quad \text{for } Pmn2_1 \qquad (10)$$

where a, b and c are the lattice parameters, u_i, v_i and w_i are integers. It can be assumed for ideal antiferromagnetic materials that the total spin system can be treated as two interpenetrating sub-lattices that have no resultant interaction between them.

Then, considering the structures shown in fig. 4 and using the values for the lattice parameter a, b and c listed in table 1, values of m_i and η_i were determined for a range of magnetic neighbors (u_i,v_i,w_i). The obtained data are given in table 2 for stannite $I\bar{4}2m$, for tetragonal pseudo cubic $P\bar{4}$ and for wurtz-stannite $Pmn2_1$ materials. Thus, using the resulting values given in table 2 together with the experimental values of a, b, c, θ and T_N listed in table 1, values of α and I_0 were determined from equations (6) and (7), and the resulting values are given in table 1. It was found that for each compound the obtained values of J_i fall very rapidly with distance r_i, and J_1 is about 2 and 5 times higher than J_2 and J_3 respectively.

Figures 5a and 5b illustrate the resulting α vs T_N/θ and (I_0/k) vs T_N/θ curves respectively. It is seen from fig. 5a that the calculated values of α for the Mn as well as for the Fe compounds lay on the same straight line. The exception being the sample Cu_2FeSnS_4, for which as indicated above, because the smallest volume gives the highest value of T_N, which yields the lowest value of α compared with the rest of the compounds. It is observed in fig. 5b that, similar to fig. 5a, the values of (I_0/k) for the Mn as well as for the Fe compounds lay on the line.

The resulting values of $-J_1/k$ versus W for the compounds are shown in fig. 6, where it is seen that the compounds with Mn lay on a different line than the one with Fe. Also, it is seen from this figure that the absolute values of $-J_1/k$ for the Fe-compounds are higher than the ones for the Mn-compounds; this result is consistent with the values of θ shown in fig. 3a. It is found that the values for the exchange constants for the present compounds are small compared to the nearest neighbor J_1/k in disordered II-VI magnetic semiconductor alloys, typically

$J_1/k \approx$ -10 K [15, 16]. Also, it is to be mentioned that, the values of θ given in fig. 3a are much smaller than those reported for the disordered zinc-blende $II_{1-x}Mn_xVI$ spin glass-like magnetic materials [17]. For the disordered zinc-blende superexchange of the type Mn-VI-Mn or Fe-VI-Fe has been found to be the dominant mechanism responsible for the magnetic interaction between nearest magnetic ions [17, 18]. This would not be the case here, since for the present ordered compounds [19] each VI anion is surrounded by two Cu, one IV and one Mn or Fe, and in this case the magnetic superexchange pathways are of the type Mn-Se….Se-Mn and/or Fe-Se….Se-Fe, and contrary to the disordered materials, no magnetic contact of the type Mn-VI-Mn or Fe-VI-Fe occurs in the ordered compounds.

The smaller values of θ for the ordered compounds would be due to the lack of superexchange of the type Mn-VI-Mn and that the closest magnetic neighbors are separated by the lattice parameter a, while for cubic zinc-blende structure the closest magnetic neighbors are separated by ($2^{1/2}a$). Furthermore, there are fewer neighbors connected by J_1, J_2 and J_3 (m_1=4, m_2=8, m_3=4, i.e. 16 magnetic atoms for ordered compounds compare to m_1=8, m_2=6, m_3=24, i.e. 38 atoms for zinc-blende materials.

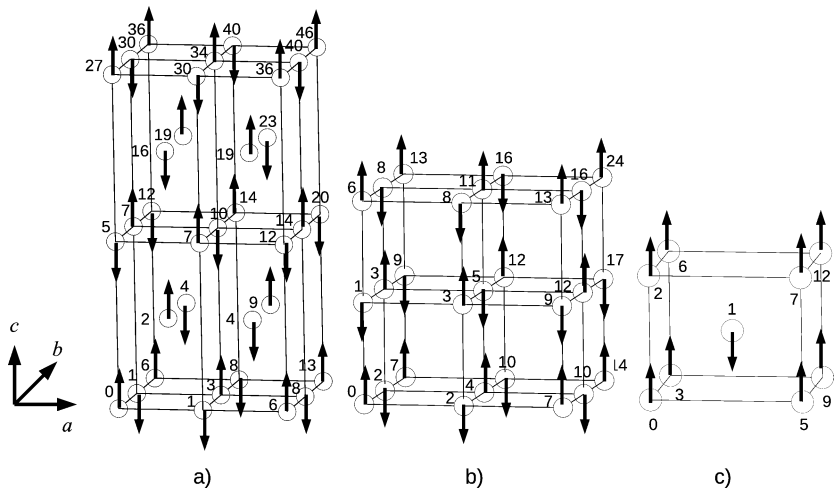

Figure 4. Magnetic unit cells showing the magnetic moments (arrows) for a) stannite $I\bar{4}2m$, with dimensions 2a, 2b, 2c, b) pseudo-cubic $P\bar{4}$ with dimensions 2a, 2b, 2c and c) wurtz-stannite $Pmn2_1$ with dimensions a, b, c structures. The numbers indicate the equidistant neighbors to magnetic ion from origin atom (zero) to i th atom in the cell. The diamagnetic ions are not shown.

Table 2. Values of i, u, v, w, m_i and η for stannite $I\bar{4}2m$, pseudo-cubic $P\bar{4}$ and wurtz-stannite $Pmn2_1$ Cu_2-II-IV-S_4(Se_4) antiferromagnetic compounds.

i	u	v	w	m_i	η	u	v	w	m_i	η	u	v	w	m_i	η
			$I\bar{4}2m$					$P\bar{4}$					$Pmn2_1$		
1	2	0	0	4	1	0	0	1	2	1	1	1	1	4	1
2	1	1	2	8	0	1	0	0	4	1	0	0	2	2	-1
3	2	2	0	4	-1	1	0	1	8	-1	0	3	0	2	-1
4	3	1	2	16	0	1	1	0	4	-1	1	-2	-1	4	1
5	0	0	4	2	1	1	1	1	8	1	2	0	0	2	-1
6	4	0	0	4	-1	0	0	2	2	-1	0	3	2	4	-1
7	2	0	4	8	-1	2	0	0	4	-1	2	0	2	4	-1
8	4	2	0	8	1	1	0	2	8	1	-1	4	1	4	1

Table 2. Cont.

i	*u*	*v*	*w*	*mi*	*η*	*u*	*v*	*w*	*mi*	*η*	*u*	*v*	*w*	*mi*	*η*
			$I\bar{4}2m$					$P\bar{4}$					$Pmn2_1$		
9	3	3	2	8	0	2	0	1	8	1	2	3	0	4	-1
10	2	2	4	8	1	2	1	0	8	1	-1	1	3	4	1
11	5	1	2	16	0	1	1	2	8	-1	1	-2	3	4	1
12	4	0	4	8	1	2	1	1	16	-1	2	3	2	8	-1
13	4	4	0	4	-1	2	0	2	8	-1	1	-5	1	4	1
14	4	2	4	16	-1	2	2	0	4	-1	-3	1	1	4	1
15	6	0	0	4	1	0	0	3	2	1	0	0	4	2	-1

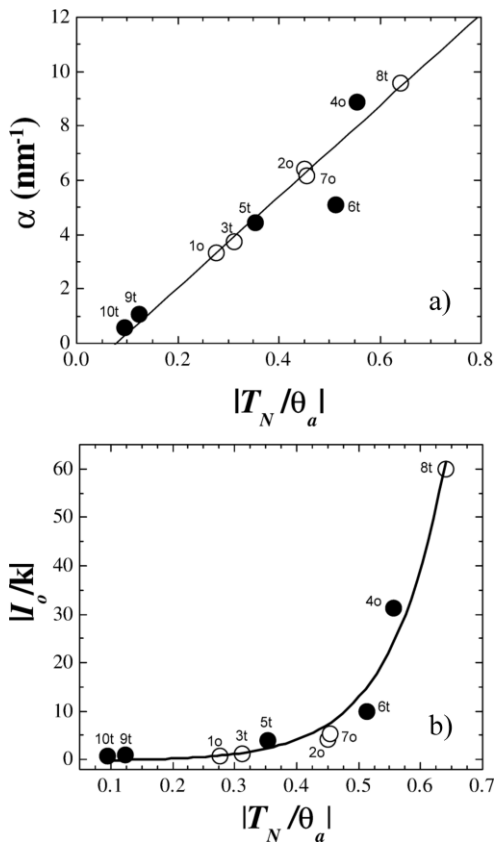

Figure 5. a) Calculated values of α as a function of the absolute value of T_N/θ. Open circles: compounds containing Mn; close circles: compounds containing Fe; t: tetragonal; o: orthorhombic. The solid lines is a linear fit given by α = 0.078+0.059 (T_N/θ). b) Calculated values of I_0/k factor as a function of the absolute value of T_N/θ. Open circles: compounds containing Mn; close circles: compounds containing Fe; t: tetragonal; o: orthorhombic. The solid lines are to guide the eyes.

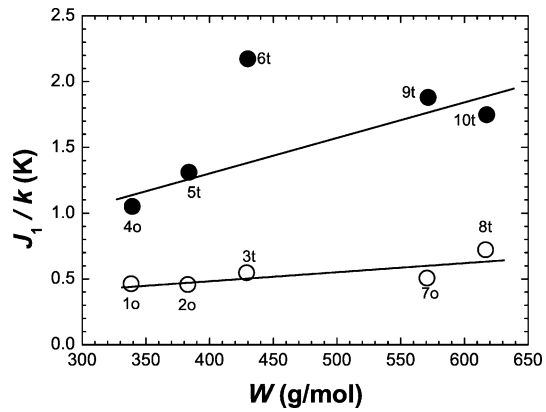

Figure 6. Dependence of the absolute value of first nearest neighbor exchange interaction J_1/k with W. Open circles: compounds containing Mn; close circles: compounds containing Fe; t: tetragonal; o: orthorhombic.

4. CONCLUSIONS

The curves of the reciprocal of the magnetic susceptibility $1/\chi$ against temperature in the range 2-300 K showed that the magnetic behavior of Cu_2MnGeS_4, Cu_2MnSnS_4, Cu_2FeSiS_4, Cu_2FeGeS_4 and Cu_2MnSiS_4 compound is antiferromagnetic. It was observed that, independent of the crystal structure of the sample, the curves of θ vs W and/or T_N vs W for the Mn and/or Fe materials, in each case, lay on different straight lines.

Using the crystal structure and lattice parameter values together with the T_N and θ experimental data, values of α and I_0/k were estimated for each compound. Hence, value for any J_i, i.e., for any *i-th* set of neighbors, could be estimated. The values of the first nearest neighbor J_1/k for the compounds

containing Mn were found to be smaller than those containing Fe. Also, it was found that independent of the crystal structure of the sample, the dependence of α against the absolute values of T_N/θ for the Mn and Fe lay on a same line, except for Cu_2FeSnS_4 for the reason given above. The exchange interaction values for the present compounds were found to be smaller than those obtained in II-VI disordered magnetic semiconductor alloys.

5. ACKNOWLEDGEMENT

This work was partially supported by the Consejo de desarrollo Científico, Humanístico, Tecnológico y de las Artes de la Universidad de Los Andes (CDCHT-ULA) (Projects No. C-1740-11-05-AA and No. C-1885-14-05-B).

6. REFERENCES

[1]. Shapira Y, McNiff EJ, Oliveira NF, Honig ED, Dwight K, Wold A. Phys. Rev. B 1988; **37**:411-418.

[2]. McCabe GH, Fries T, Liu MT, Shapira Y, Ram-Mohan LR, Kershaw R, Wold A, Fau C, Averous M, McNiff EJ. Phys. Rev. B 1997; **56**:6673-6680.

[3]. Shafer W, Nitsche R. Mater. Res. Bull. 1974; **9**:645-654.

[4]. Gulay LD, Nazarchuk OP, Olekseyuk ID. J. Alloy Compd. 2004; **377**:306-311.

[5]. Llanos J, Tapia M, Mujica C, Oro-Sole J, Gomez-Romero P. Bol. Soc. Chil. Quim. 2000; **45:**605. ICDD powder diffraction file No. 01-070-4373. http://dx.doi.org/10.1016/j.jallcom.2004.02.004

[6]. Quintero M, Moreno E, Alvarez S, Marquina J, Rincón C, Quintero E, Grima-Gallardo P, Henao JA, Macías MA. Rev. LatinAm. Metal. Mat. 2014; **34:**28-38.

[7]. Chen XL, Lamarche A-M, Lamarche G and Woolley JC. Journal of Magnetism and Magnetic Materials 1993; **118**:119-128.

[8]. Quintero E, Tovar R, Quintero M, González J, Broto JM, Rakoto H, Barbaste R, Woolley JC, Lamarche G, and Lamarche AM. J. Magn. Magn. Mater. 2000; **210**:208-214.

[9]. Smart JS. Effective Field Theory of Magnetism, Saunders Company, Philadelphia & London, 1966.

[10]. Quintero E, Quintero M, Moreno E, Lara L, Morocoima M, Pineda F, Grima-Gallardo P, Tovar R, Bocaranda P, Henao JA, and Macías MA. J Phys. Chem. Solids 2010; **71**:993-997.

[11]. Quintero E, Tovar R, Quintero M, Morocoima M, Ruiz J, Delgado G, Broto JM, and Rakoto R. Physica B 2002; **320**:384.

[12]. Woolley JC, Bass S, Lamarche AM, and Lamarche G. J. Magn. Magn. Mater. 2000; **210**:208-214.

[13]. Geertsma W, Hass C, Sawatzky GA and Vertogen G. Physica B 1977; **1039**:86-88.

[14]. Concalves da Silva CET and Falicov LM. J. Physique C. 1973; **5**:142-145.

[15]. Larson BE, Hass KC, Ehrenreich H, and Carlsson AE. Phys. Rev. B 1988; **37**:4137.

[16]. Shapira Y. J. Appl. Phys. 1990; **67**:5090. http://dx.doi.org/10.1063/1.344682

[17]. Furdyna JK and Kossut J. Diluted Magnetic Semiconductors, Semiconductors and Semimetals, (Edited by Willardson R. K. and Beer A. C.), Vol. 25, Chap. 1., Academic Press, New York. (1988).

[18]. Spalek J, Lewicki A, Tarnawski Z, Furdyna JK, Galazka RR, and Obuszko. Z. Phys. Rev. B 1986; **33**:3407-3418.

[19]. Quintero E, Quintero M, Moreno E, Morocoima M, Grima-Gallardo P, Bocaranda P, Henao JA, Pinilla J. Journal of Alloys and Compounds 2009; **471**:16–20.

©2017 Universidad Simón Bolívar